

## Full Length Article

# Simple surface modification of poly(methyl methacrylate) microfluidic microplates for enhanced ultrasensitive multiplexed detection of infectious diseases

Sharma T. Sanjay<sup>a</sup>, Sapna Kannan<sup>a</sup>, XiuJun Li<sup>a,b,\*</sup>

<sup>a</sup> Department of Chemistry and Biochemistry, University of Texas at El Paso, 500 West University Ave, El Paso, TX, 79968, USA

<sup>b</sup> Border Biomedical Research Center, Forensic Science, & Environmental Science and Engineering, University of Texas at El Paso, 500 West University Ave, El Paso, TX, 79968, USA

## ARTICLE INFO

## Keywords:

Colorimetric ELISA  
Surface modification of poly(methyl methacrylate)  
Polylysine  
Microfluidic microplate  
Infectious diseases  
Hepatitis B virus

## ABSTRACT

Novel strategies for the simultaneous and portable detection of multiple analytes are highly favorable for clinical diagnosis and healthcare. Conventional colorimetric enzyme-linked immunosorbent assay (ELISA) is a widely used laboratory technique for medical diagnostics, quality control, and research applications. However, nonspecific absorption of proteins may lead to a reduction of functional sites, resulting in high background and low sensitivity in ELISA. Herein, we report a simple method of functionalization of poly(methyl methacrylate) (PMMA) with polylysine to be used as the microfluidic microplate substrate for enhanced ELISA, enabling rapid, ultrasensitive, and multiplexed detection of infectious diseases. FTIR and fluorescence microscopy characterization confirmed high amine densities on polylysine-modified PMMA surface, resulting in high detection sensitivity of the colorimetric ELISA on the PMMA microdevice. The ultrasensitive polylysine-modified microplate can immobilize protein within 20 min and results of the assay can be viewed by the naked eye or scanned through a simple desktop scanner for quantitative analysis within 90 min. A sandwich-type immunoassay for the rapid and sensitive detection of immunoglobulin G (IgG), hepatitis B surface antigen (HBsAg), and hepatitis B core antigen (HBcAg) was demonstrated as a proof-of-concept for multiplexed detection. The limits of detection (LOD) of 200.0 pg/mL for IgG, 180.0 pg/mL for HBsAg, and 300.0 pg/mL for HBcAg were achieved, without any specialized equipment like a microplate reader. The surface-modified microchip exhibited about 10-fold higher sensitivity than traditional microplates. This surface-modified microplate has tremendous potential as a point-of-care multiplexed testing platform for many applications ranging from clinical diagnosis to environmental monitoring, particularly in resource-limited settings.

## 1. Introduction

Infectious diseases including SARS and COVID-19 have been the major cause of death and mortality along with high disability rates throughout the world, roughly accounting for 15 million deaths per annum [1–5]. We are currently in a very fragile balance with respect to the continual emergence of new infectious diseases such as COVID-19 and the re-emergence of old infectious diseases, together with the potential for their global spread [6–8]. Infectious diseases stand out among many challenges to health because of their profound impact on human species and unpredictable and explosive global effects due to their pandemics [2,7]. For instance, Hepatitis B virus (HBV), one of the major causes of chronic

hepatitis damage and hepatocellular carcinoma has approximately 2 billion infection cases with 1.2 million deaths every year [9–11]. 5%–15% of the people in developing and underdeveloped countries carry HBV, which is one of the leading causes of chronic hepatitis with more than 350 million current carriers [12]. In addition, chronic hepatitis B (CHB) is the leading risk factor for hepatocellular carcinoma, which results in 746,000 deaths per year [2]. This underlines the need for accurate surveillance and the development of new strategies for rapid and sensitive detection of infectious diseases for their control [13].

Enzyme-linked immunosorbent assay (ELISA) is one of the most widely used laboratory assays for the detection of infectious diseases, cancer, and other biomolecules [14–17]. The traditional ELISAs are

This article is part of a special issue entitled: Biosensors and Energy Materials published in Advanced Sensor and Energy Materials.

\* Corresponding author. Department of Chemistry and Biochemistry, University of Texas at El Paso, 500 West University Ave, El Paso, TX, 79968, USA.

E-mail address: [xli4@utep.edu](mailto:xli4@utep.edu) (X. Li).

<https://doi.org/10.1016/j.asems.2025.100142>

Received 17 December 2024; Received in revised form 16 February 2025; Accepted 16 February 2025

Available online 28 February 2025

2773-045X/© 2025 The Author(s). Published by Elsevier B.V. on behalf of Changchun Institute of Applied Chemistry, CAS. This is an open access article under the CC BY-NC-ND license (<http://creativecommons.org/licenses/by-nc-nd/4.0/>).

limited due to long incubation periods (overnight incubation), labor-intensive methods, consumption of significant volumes of samples and reagents, requirement of laboratory settings, and complicated and expensive instruments including robotic pipettors, washers, and microplate reader [7,18,19]. For instance, Shen et al. developed an electrochemical method for detecting hepatitis B surface antigen (HBsAg), which required complicated and time-consuming preparation of conjugates and nanoparticles, along with an assay time of nearly 16 h, similar to conventional ELISA [20]. Therefore, a point-of-care (POC) microarray device for rapid and sensitive multiplexed detection of infectious diseases remains a challenge [21,22].

Modern analytical chemistry and clinical diagnosis have greatly advanced POC testing, a critical area for *in vitro* diagnostics [23,24]. To address this need, microfluidic devices serve as a promising POC diagnostic tool, facilitating both quantitative and qualitative detection of analytes without the need for any specialized equipment [25–30]. Microfluidic devices with remarkable features including rapid analysis, high surface-to-volume ratio, portability, integrated processing, and consumption of microliter of samples result in low-cost, minimal reagent consumption, and rapid bioanalysis of complex biological fluids for detection of infectious diseases, forensic analysis along with cells and tissue culture analysis, and drug delivery [31–39]. Different kinds of substrates including polydimethylsiloxane (PDMS), poly(methyl methacrylate) (PMMA), and paper have been used as cost-effective microfluidic substrates for the detection of infectious diseases [40–44]. Paper-based devices have lower sensitivity; they are not uniform and have low performance in flow control [44,45]. PMMA is a low-cost, rigid, and transparent substrate, which is easier to fabricate and mass-produce than PDMS [46]. It also offers better performance under mechanical stress as compared to PDMS. PMMA has been used to perform ELISA but it shows low sensitivity as hydrophobic PMMA surface lacks functional groups to immobilize proteins and thus requires complex surface modifications and detection techniques [47,48].

Sensitivity and background noise of the biochemical assays are profoundly affected by the total activity and the way of interaction of the specific protein/enzyme bound to the surface of the assay substrate [49]. In addition, the way of interaction is very sensitive towards their environment and can easily lose their activity as they are brought in close proximity to the solid surfaces [47]. The hydrophobic physical adsorption of proteins onto the microfluidic surface may reduce functional sites or activities of the protein by even more than 90% and may result in strong non-specific binding and high background noise [50]. To increase the sensitivity and binding efficiency of the microfluidic chip, an appropriate surface modification is crucial [44,50–55]. For instance, Brown et al. modified the PMMA surface using air plasma, acid-catalyzed hydrolysis, and aminolysis (using ethylenediamine) to determine if the covalent and/or hydrogen bonds between modified PMMA substrate and cover plate increase their adhesion [52]. However, this PMMA surface modification method using air plasma, acid-catalyzed hydrolysis, and acid hydrolysis was mainly used to enhance chip bonding, and has not been used for covalent immobilization of proteins for immunosensing. Bai et al. studied the surface modification of PMMA to enhance the antibody binding on the polymer-based microfluidic device to perform ELISA. They modified the base-treated PMMA by immersing in poly(ethyleneimine) (PEI) followed by treatment with glutaraldehyde, and found that the PEI-modified PMMA was 10 times more active in binding antibodies as compared to those without treatment or treated with a small amine-bearing molecule, hexamethylenediamine (HMD) [50]. They performed the ELISA of immunoglobulin G (IgG), but only achieved a similar detection limit as the conventional 96-well plate. To achieve better sensitivity, Liu et al. developed an electrochemical detection method on a PEI-modified PMMA chip for the detection of  $\alpha$ -fetoprotein (AFP), a hepatocellular carcinoma biomarker [54]. However, their detection system requires syringe pumps and an expensive electrochemical analyzer.

In addition, Llopis et al. studied the surface modification of PMMA microfluidic devices for the separation of single-stranded DNA [53]. They created an amine-terminated PMMA surface by the chemical or

photochemical process by using ethylenediamine, which was then used to covalently anchor methacrylic acid as a scaffold to produce linear polyacrylamides (LPAs). Although PMMA has been functionalized with different methods for various purposes including ELISA, these methods usually require complex surface modification procedures, unstable intermediates, non-environment-friendly solvents, and costly and bulky detection equipment for subsequent detection, because they usually do not provide high detection sensitivity due to low amine density, making it challenging for them to be adopted for microfluidic POC analysis.

In response to the aforementioned challenges, herein, we report a simple method of functionalizing PMMA surface with polylysine resulting in high amine density. Modified PMMA has been used as a microfluidic device substrate for enhanced ELISA for high sensitivity multiplexed detection of disease biomarkers. A 64-microwell microplate with an  $8 \times 8$  series, designed according to a standard 384-well ELISA plate with the same X-axis and Y-axis offset but with reduced diameter and depth, was fabricated with a laser cutter so that the working volume could be decreased to 5  $\mu$ L. Two different methods of functionalizing PMMA were compared against plasma-treated PMMA and pristine PMMA for colorimetric immunoassays. Covalent binding of antibody/antigen with glutaraldehyde to the amine-dense microplate resulted in significant improvement of sensitivity and a decrease in the background noise as compared to traditional microplates. Antibody/antigen could be immobilized in the surface-modified PMMA within 20 min as compared to overnight incubation in traditional microplates due to the enhanced binding efficiency of protein. This surface-modified PMMA microdevice provides a low-cost platform for sensitive, rapid, and high-throughput multiplexed assay of multiple infectious disease biomarkers including HBsAg, hepatitis B core antigen (HBcAg), and IgG. Results of the ultrasensitive assay can be viewed by naked eye within 90 min or scanned through the desktop scanner for quantitative analysis without the use of any sophisticated instruments. As a proof-of-concept, sandwich-type multiplexed detection of IgG, HBsAg, and HBcAg was achieved with the limits of detections (LODs) of 200.0 pg/mL, 180.0 pg/mL, and 300.0 pg/mL, respectively, which is about 10-fold more sensitive than traditional ELISA. Since the detection approach does not require costly and bulky instruments, this surface-modified PMMA microchip is advantageous for ultrasensitive POC detection of multiple low-concentration disease biomarkers from infectious diseases to cancer, especially in low-resource settings.

## 2. Experimental section

### 2.1. Chemicals and materials

IgG from rabbit serum, Tween 20, albumin from bovine serum, anti-rabbit IgG-alkaline phosphatase, BCIP/NBT liquid substrate, polylysine, sodium hydroxide, dimethylsulfoxide, and Phosphate Buffer Saline were purchased from Sigma Aldrich (St. Louis, MO). HBsAg protein (subtype ad) was purchased from Fitzgerald Industries International Inc., Acton, MA. Polyclonal anti-HBsAg was purchased from Novus Biologicals, Littleton, CO. Hepatitis B virus core antigen and anti-hepatitis B virus core antigens were obtained from Fisher Scientific (Hampton, NH). Glutaraldehyde was purchased from Amresco, Solon, OH. Isopropyl alcohol was purchased from J.T. Baker, Center Valley, PA. PMMA was purchased from McMaster-Carr, Los Angeles, CA. Ultrapure Milli-Q water (18.2 M $\Omega$  cm) obtained from a Millipore water purification system (Bedford, MA) was used in all assays and reagent preparation unless otherwise noted.

### 2.2. PMMA microplate platform design and fabrication

The microfluidic microplate used in this study was designed in Adobe Illustrator CS5 and micro-machined using a 30 W CO<sub>2</sub> Laser cutter in the raster mode with a speed of 30% and power of 65% (Epilog Zing 16, Golden, CO). The wells in the PMMA layer are designed according to the

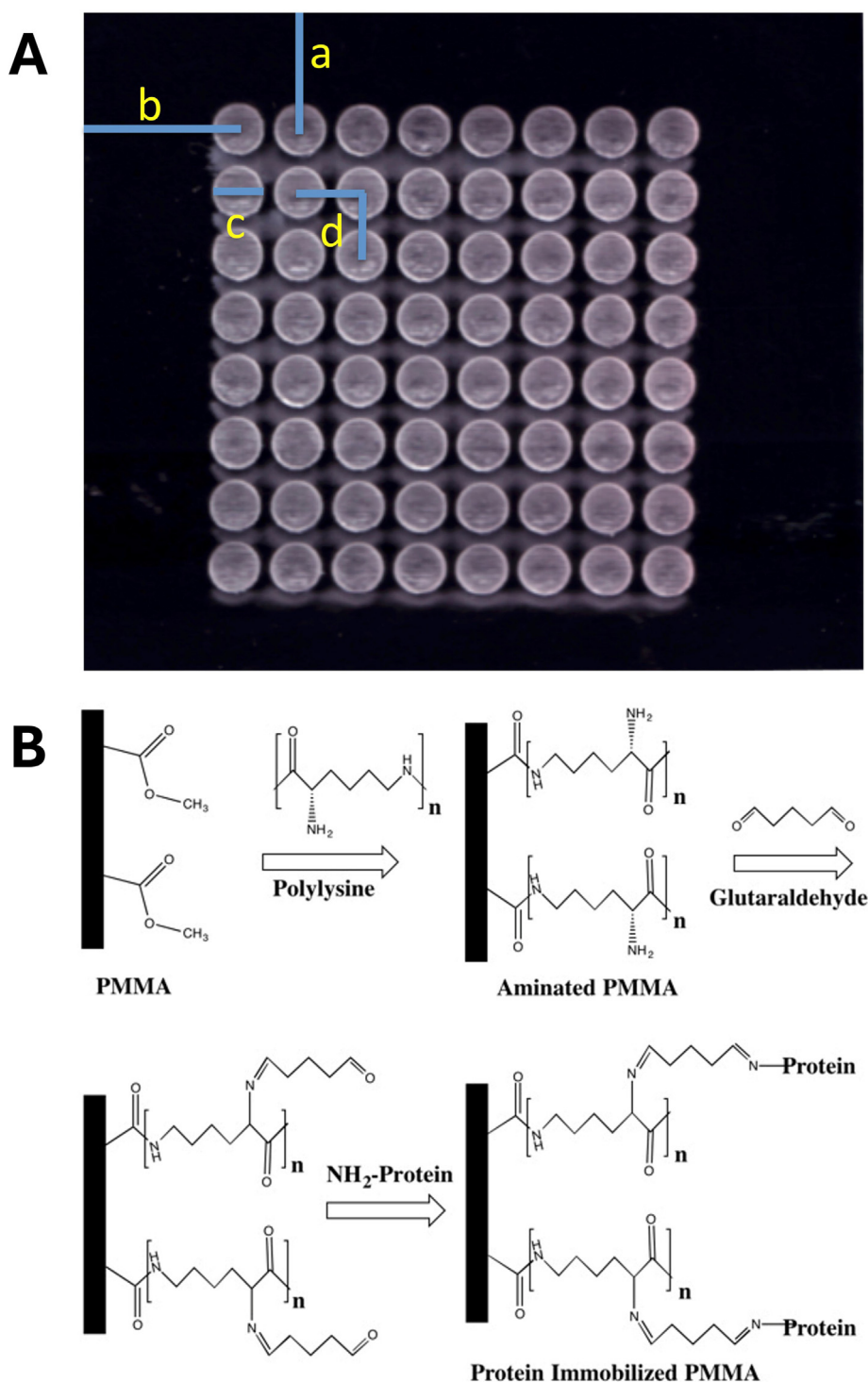


**Fig. 1.** PMMA microplate platform design and surface modification. (A) Photograph of the actual device with a black background. (B) Schematic representation of covalent modification of PMMA.

dimensions of a standard 384 well plate. As seen from Fig. 1A, the X-axis and Y-axis offset are 4.5 mm (d), which is the length between the centers of 2 wells. The position of the first well corresponds to A1 of a microtiter plate. A1 row offset (distance from the top edge of the microplate to the center of wells in 1st row) of the chip is 8.99 mm (a), similar to 384 well microtiter plate. In addition, A1 column offset (distance from the side edge of the microplate to the center of wells in the 1st column) of 12.13 mm (b) is also the same as a microtiter plate. The diameter of each well is 3.6 mm (c).

### 2.3. Covalent modification of PMMA surface

PMMA was functionalized using two different methods, where aminolysis of PMMA surface was achieved using polylysine followed by activation using glutaraldehyde for the covalent modification of antigen/antibody (Fig. 1B), with the major differences in the PMMA surface treatment before polylysine treatment. In the first method, PMMA was sonicated for 5 min in 40% by volume of aqueous 2-propanol solution.

After the PMMA was dried, PMMA was immersed in 0.2% (v/v) polylysine in dimethyl sulfoxide (DMSO) for 20 min at room temperature followed by rinsing in 2-propanol solution. Finally, the aminated PMMA was immersed in glutaraldehyde solution (1% v/v) at room temperature for 30 min. Glutaraldehyde which acts as a cross-linker forms the Schiff base with the amine group of polylysine. The glutaraldehyde-activated PMMA was washed once with phosphate-buffered saline (PBS) and used for the immobilization of antigen/antibody by forming a Schiff base at the other end of glutaraldehyde. ELISA was performed on this covalently linked protein.

In the second method, PMMA was immersed in 1 N sodium hydroxide (NaOH) solution at 55 °C for 30 min to obtain a hydrophilic –OH group followed by immersing in 0.2% polylysine in water at room temperature with pH of 7 for 1 h to get aminated PMMA. After the aminolysis, PMMA was immersed for 30 min in 1% v/v glutaraldehyde solution at room temperature. Similar to the first method, the surface-modified PMMA was used for the immobilization of antigen/antibody, followed by ELISA procedure after washing it once with PBS.

#### 2.4. FTIR analysis of modified PMMA surface

FTIR-spectroscopy was used for the characterization of PMMA surface modification by an FTIR spectrometer, PerkinElmer Spectrum 100. PMMA was first cut into 1 cm × 1 cm square pieces by using a laser cutter in raster mode with speed of 10% and power of 50%. Then the PMMA was laser ablated to obtain wells with a diameter of 3.6 mm. The FTIR spectra were recorded after each modification step for both the modification procedure to characterize specific functional groups. FTIR spectra were taken for pristine PMMA, PMMA + polylysine, PMMA + polylysine + glutaraldehyde, and PMMA + polylysine + glutaraldehyde + antibody.

#### 2.5. Verification of protein immobilization using fluorescence microscopy

Unspecific absorption of proteins often leads to a reduction of functional sites and an increase in the background signal, resulting in lower immobilization of proteins and low sensitivity of the assay. Fluorescence microscopy was used to show higher immobilization efficiency of antigen/antibody on the modified PMMA surfaces as compared to pristine PMMA and plasma-treated PMMA. Five different sets of PMMA were taken and microwells were created using the laser cutter. 20 µg/mL of Cy3 IgG was added to surface-modified PMMA (both methods), plasma-treated PMMA, and pristine PMMA to see their protein immobilization efficiency. Cy3 IgG was not added to one set of PMMA to see the background fluorescence of PMMA. For plasma treatment of the PMMA, the laser-ablated PMMA was placed in a plasma cleaner (PDC-32G, Harrick Plasma, NY, USA) for 1 min. PMMA devices were incubated for 20 min with Cy3 IgG and then washed three times with phosphate-buffered saline with Tween 20 (PBST) before measuring the fluorescence intensity using a Nikon Ti-E fluorescence microscope (Melville, NY).

#### 2.6. Sandwich-type ELISA for the colorimetric detection of infectious disease biomarkers on PMMA microdevices

The surface-modified PMMA was used for the ELISA of different biomarkers for infectious diseases including IgG, HBsAg, and HbCag. For the ELISA of IgG, the rabbit IgG was used as the analyte. To each well 5 µL of serially diluted standard samples of IgG ranging from 0.1 ng/mL to 100 µg/mL in 10 mM pH 8.0 PBS were added. Each concentration had eight replicas along the same column of the chip. IgG solutions were prepared from the stock solution of 2 mg/mL IgG. The chip was incubated at room temperature for 20 min. Following the reaction, bovine serum albumin (4.5% BSA w/v in PBS + 0.05% Tween 20) was added for 20 min to block the unreacted surface of the PMMA. Next, the microplate chip was thoroughly washed with 8 µL of washing buffer PBST (10 mM, pH 7.4 PBS + 0.05% Tween 20) to get rid of unbound proteins. After washing, 5 µL of enzyme-

linked antibody, i.e., anti-rabbit IgG-alkaline phosphatase (6 µg/mL) was added and incubated at room temperature for 7 min. Finally, the chip was thoroughly washed with PBST three times and 5 µL of the substrate, BCIP/NBT (5-bromo, 4-chloro, 3-indoyl phosphate + nitroblue tetrazolium) was added. The substrate, which is initially light yellow in color, is converted to insoluble dark purple NBT diformazan as the end product which can be observed visually by the naked eye. Following 10 min of incubation with the substrate, an office scanner was used to scan the chip. Quantitative detection was carried out using the free software ImageJ by measuring the brightness value of each microwell of the microplate.

HBsAg and HbCag were used as two biomarkers for the detection of HBV and a similar assay procedure as IgG was followed. For the detection of HBsAg, first, the antigen, i.e., HBsAg, was immobilized on the modified surface of PMMA. After the antigen was incubated for 20 min, the blocking buffer was added for another 20 min. The incubation was followed by thorough washing with PBST and the addition of anti-HBsAg for another 20 min. Finally, after washing it with the washing buffer three times, a sandwich-structure immunoassay was formed by the addition of alkaline phosphatase (ALP)-labelled anti-rabbit IgG. Similar to the detection of HBsAg, for the detection of HbCag, anti-HbCag was added after the initial immobilization of HbCag. Finally, ALP-labelled anti-rabbit IgG was added to form a sandwich immunoassay. The microplate was scanned 10 min after the addition of the substrate BCIP/NBT in both cases.

#### 2.7. Multiplexed detection of HBsAg and HbCag on PMMA microdevices

The surface-modified PMMA microdevice can be simultaneously used for high-sensitivity detection of multiple disease biomarkers. Here, the microdevice has been used for multiplexed detection of HBsAg and HbCag, two major biomarkers for the detection of HBV. This experiment also serves the purpose of specificity for the detection of HBsAg and HbCag. The first column of the microdevice is for negative controls with PBS and no antigen. HBsAg was immobilized in the second and third columns, HbCag was immobilized in the fourth and fifth columns, while both HBsAg and HbCag were immobilized in the sixth, seventh, and eighth columns. Different combinations of antigens as mentioned above were incubated for 20 min and then blocking buffer was added for another 20 min followed by a thorough washing with the washing buffer. After that, anti-HBsAg was added in the second, fourth, and seventh columns; anti-HbCag was added in the third, fifth, and eighth columns while both anti-HBsAg and anti-HbCag were added in the first and sixth columns. After the primary antibodies were incubated for 20 min, the ALP-labelled secondary antibody was added and incubated for another 7 min. Finally, the microdevice was scanned using a desktop scanner, 10 min after the addition of the substrate.

### 3. Results and discussions

#### 3.1. FTIR characterization of modified PMMA surface

As we can see from the FTIR spectrum of PMMA in Fig. 2, there is a distinct absorption band from 1150 to 1250 cm<sup>-1</sup>, which can be attributed to the C–O–C stretching vibration. The two bands at 1387 and 750 cm<sup>-1</sup> can be attributed to the α-methyl group vibrations. The band at 986 cm<sup>-1</sup> is the characteristic absorption vibration of PMMA, together with the bands at 1063 and 841 cm<sup>-1</sup>. The band at 1723 cm<sup>-1</sup> shows the presence of the acrylate carboxyl group. The band at 1435 cm<sup>-1</sup> can be attributed to the bending vibration of the C–H bonds of the –CH<sub>3</sub> group. The two bands at 2995 and 2951 cm<sup>-1</sup> can be assigned to the C–H bond stretching vibrations of the –CH<sub>3</sub> and –CH<sub>2</sub>– groups, respectively. This spectrum correlates well with the FTIR spectrum of PMMA that has been documented in the literature [56].

Some major changes can be observed in the spectrum of PMMA once it has been modified using method 1 (Fig. 2A). The presence of Amide I (1652 cm<sup>-1</sup>), Amide II (1533 cm<sup>-1</sup>), and C–N stretch, as well as substantially less intense methyl ester bands after the treatment of PMMA with polylysine, shows that the PMMA was aminated by polylysine.

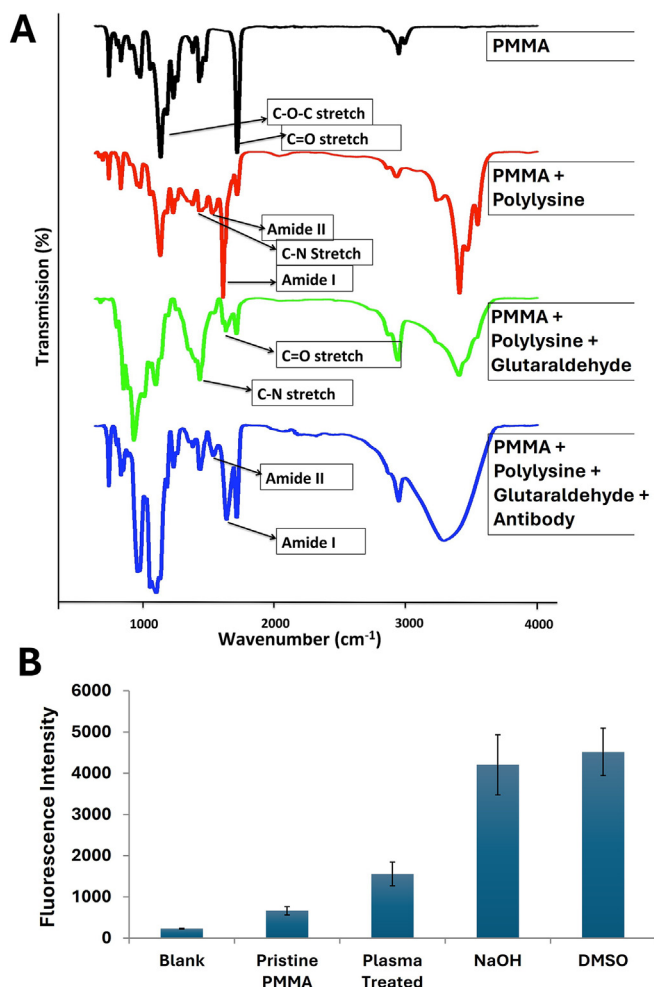


**Fig. 2.** Characterization of surface-modified PMMA. (A) FTIR characterization of modified PMMA surface (modification method #1). (B) Fluorescence intensity of Cy3 IgG immobilized on the surface modified PMMA. DMSO and NaOH in (B) represent methods #1 and #2, respectively ( $n = 3$ ).

These data suggest that the ester bond of PMMA is replaced by the amide bond of polylysine as found in the literature for amine-modified PMMA [56]. The aminated PMMA was further treated with glutaraldehyde to covalently bind the antibody to the PMMA surface, as can be seen from C=O ( $1637\text{ cm}^{-1}$ ) and C-N ( $1442\text{ cm}^{-1}$ ) stretch vibrations. Strong absorption for Amide I ( $1646\text{ cm}^{-1}$ ) and Amide II ( $1555\text{ cm}^{-1}$ ) was observed after the addition of the antibody, which confirmed the covalent binding of the antibody to the modified PMMA surface.

Some major changes can also be observed in the spectrum of PMMA once it was treated with NaOH to get a hydroxyl group followed by treatment with polylysine to get aminated PMMA (method 2, Fig. S1). The presence of Amide I ( $1617\text{ cm}^{-1}$ ), Amide II ( $1534\text{ cm}^{-1}$ ) and C-N ( $1435\text{ cm}^{-1}$ ) stretch after the treatment of PMMA with polylysine shows that the PMMA was aminated by polylysine. Also, the  $-\text{CH}_2$  stretching mode of vibration at  $2933\text{ cm}^{-1}$  and the V1 proton mode band of the peptide at  $3239\text{ cm}^{-1}$  were observed. The aminated PMMA was further treated with glutaraldehyde, as can be seen from C=O ( $1637\text{ cm}^{-1}$ ) and C-N ( $1440\text{ cm}^{-1}$ ) stretch vibration. We can see strong absorption for Amide I ( $1643\text{ cm}^{-1}$ ) and Amide II ( $1541\text{ cm}^{-1}$ ) after the addition of the antibody, which proves the presence of amine functionalities of the antibody due to the electrostatic interaction to the modified PMMA surface. When comparing Method #1 and #2, a much more intense Amide I band, and C-N stretch were observed after modification using Method #1 implying that Method #1 could generate more amine-modified PMMA. Subsequent treatment with glutaraldehyde gave intense C-N stretch in

method #1 followed by intense Amide I and Amide II band for method #1 after adding antibodies, which indicates that method #1 is more efficient for covalently binding the antibody to the PMMA surface. In method 1, the organic solvent DMSO is used which could partially penetrate and swell PMMA and interact more extensively with ester groups, resulting in more reactive sites and higher degree of covalent modification and amine group density. Whereas, in method 2, NaOH hydrolyzes the ester group to carboxylate and hydroxyl groups with negative charge. When polylysine is added afterwards, it mainly binds to the negatively-charged PMMA surface through the electrostatic interaction rather than covalent binding which could lead to lower density of stable amine groups.

### 3.2. Validation of protein immobilization using fluorescence microscopy

After FTIR characterization, fluorescence microscopy was utilized to assess the modification and the differences in the antibody immobilization between the modified PMMA and the pristine PMMA. After the surface modification or plasma treatment of PMMA,  $20\text{ }\mu\text{g/mL}$  of Cy3 IgG was added to corresponding microwells and incubated for 20 min for the measurement of fluorescence intensity. Fig. 2B shows that polylysine-modified PMMA (both methods 1 and 2) gives around seven-fold higher fluorescence intensity as compared to the pristine PMMA, indicating enhanced immobilization efficiency of the antibody. Method 1 gave slightly higher intensity as compared to method 2, which was consistent with FTIR characterization, but the increase in intensity/immobilization was insignificant. We can also observe a threefold increase in the fluorescence intensity of the polylysine-modified PMMA, as compared to plasma-treated PMMA. The blank represented a small background fluorescence intensity of PMMA without the addition of Cy3 IgG. The result shows that the immobilization efficiency of protein was significantly increased because of the surface modification of the PMMA, which may ultimately lead to an increase in the sensitivity of ELISA.

### 3.3. Sandwich-type ELISA for the detection of infectious disease biomarkers on polylysine-modified PMMA microplates

To demonstrate the feasibility of the detection of infectious disease biomarkers, we performed the colorimetric ELISA for the detection of IgG. IgG, the most common antibody in the human blood, can be used for diagnosis of autoimmune hepatitis and Neuromyelitis Optica [57,58]. We performed ELISA of IgG with 10-fold diluted concentrations ranging from  $100\text{ }\mu\text{g/mL}$  to  $0.1\text{ ng/mL}$ . Each of the microwells just required  $5\text{ }\mu\text{L}$  of the sample and each concentration had 8 repeats, as seen in Fig. 3. The chip was scanned 10 min after the addition of the substrate and we can see the increasing intensities of purple from the left to right in Fig. 3A—as the concentration increases from  $0.1\text{ ng/mL}$  to  $100\text{ }\mu\text{g/mL}$ . Fig. 3B shows the calibration curve for the detection of IgG by plotting corrected brightness against the concentrations of IgG. The calibration curve of IgG on surface-modified PMMA (method #1) was linear over the range of  $10^2\text{ pg/mL}$  to  $10^6\text{ pg/mL}$  with a regression curve of  $y = 9.72\text{ log}(x) + 98.95$  ( $R^2 = 0.98$ ). The LOD is defined as the concentration value that generates a signal three standard deviations above the blank value. The LOD of IgG on surface-modified PMMA (method #1) was found to be  $200.0\text{ pg/mL}$ . Similar to the detection of IgG in surface-modified PMMA (method #1), the calibration curve of IgG on surface-modified PMMA (method #2) was linear over the range of  $10^2$  to  $10^7\text{ pg/mL}$  with a regression curve of  $y = 12.26\text{ log}(x) + 42.49$  ( $R^2 = 0.98$ ). The LOD of IgG on surface-modified PMMA (method #2) was found to be  $140.0\text{ pg/mL}$  (Fig. S2). The LOD of IgG was found to be more than 10-fold sensitive as compared to commercial 96-well microplate ELISA (LOD,  $1.6\text{--}6.25\text{ ng/mL}$ ) without the use of any specialized instrument like a microplate reader [59]. In addition, our microplate just requires  $5\text{ }\mu\text{L}$  of sample and 90 min of assay time, compared to  $50\text{--}100\text{ }\mu\text{L}$  of sample and 18 h of assay time in a traditional microplate. Our surface-modified device is also more sensitive as compared to APTES-modified PMMA (12 h incubation time and LOD of  $0.12\text{ }\mu\text{g/mL}$ ) [49], paper-based device (54

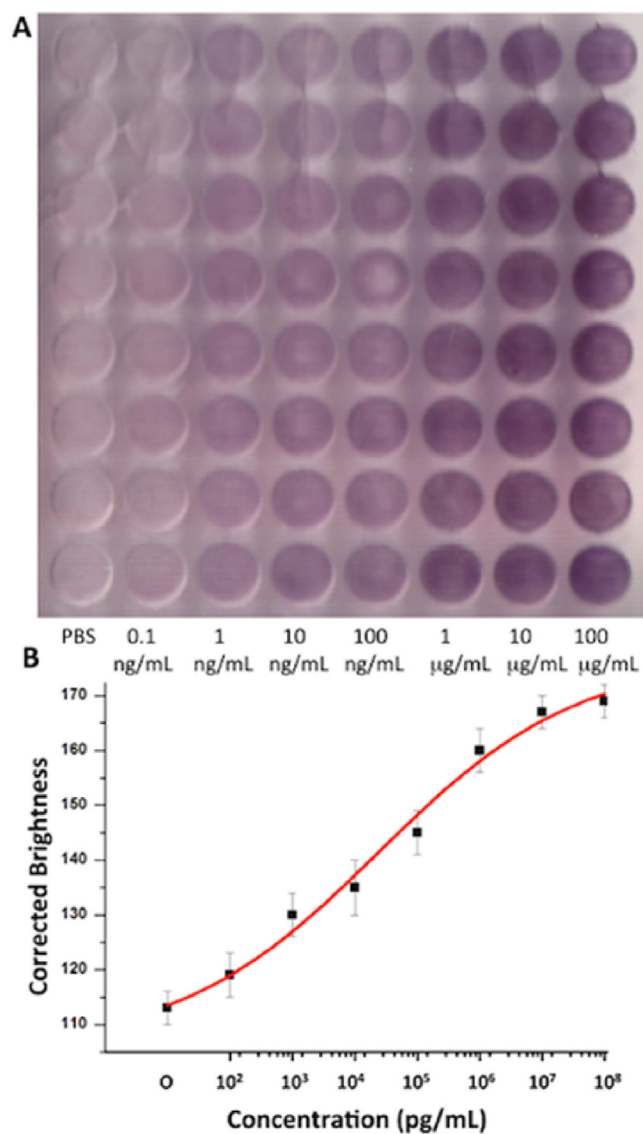


**Fig. 3.** Detection of IgG on surface-modified PMMA microplates (method #1). (A) Scanned image of enzymatic converted substrate in different columns of the microplate with concentrations from left to right: blank (0 pg/mL), 0.1 ng/mL, 1 ng/mL, 10 ng/mL, 100 ng/mL, 1  $\mu$ g/mL, 10  $\mu$ g/mL, and 100  $\mu$ g/mL, respectively. (B) The sigmoidal curve of the corrected brightness of IgG over a concentration range of  $10^2$  to  $10^8$  pg/mL ( $n = 8$ ).

f/mol/zone) [45], and our previous hybrid device (LOD, 1.6 ng/mL) [60]. Bai et al. also used amine-bearing poly(ethyleneimine) to modify the PMMA but got the LOD only comparable to that of a 96-well plate method and the linear dynamic range from 5 to 500 ng/mL even with the use of a fluorescence microscope [50].

For the detection of HBV, HBsAg and HbcAg were used as its biomarkers. HBsAg has been mainly used for the diagnosis and remission of hepatitis B [61,62]. To detect HBsAg, the antigen HBsAg was first immobilized on the surface-modified PMMA microwells, followed by the addition of the primary antibody, anti-HBsAg, and the secondary antibody (goat anti-rabbit IgG) conjugated with ALP. Finally, the enzymatic reaction between ALP and the colorimetric substrate BCIP/NBT produced the purple color, similar to the detection of IgG. The calibration curve of HBsAg on surface modified PMMA (method #1) was linear over the range of  $34 \times 10^1$  to  $34 \times 10^6$  pg/mL with a regression curve of  $y = 13.13 \log(x) + 75.1$  ( $R^2 = 0.98$ ). The LOD of HBsAg on surface-modified PMMA (method #1) was found to be 180.0 pg/mL (Fig. 4). Similarly,

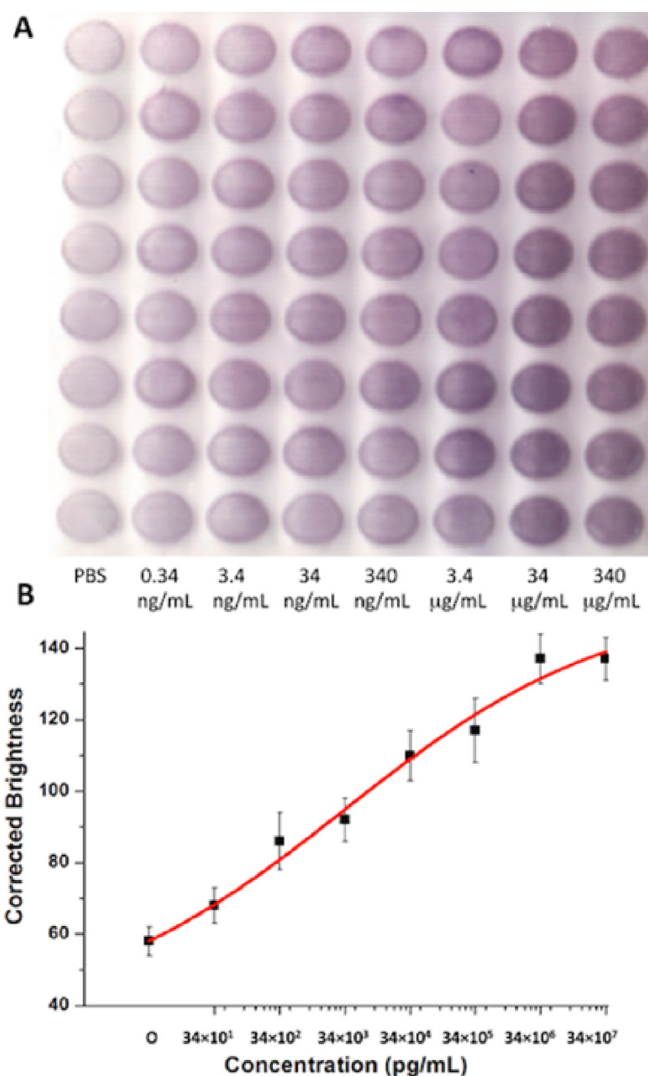


**Fig. 4.** Detection of HBsAg on surface-modified PMMA microplates (method #1). (A) Scanned image of enzymatic converted substrate in different columns of the microplate with concentrations, from left to right: blank (0 pg/mL), 0.34 ng/mL, 3.4 ng/mL, 34 ng/mL, 340 ng/mL, 3.4  $\mu$ g/mL, 34  $\mu$ g/mL, and 340  $\mu$ g/mL, respectively. (B) The sigmoidal curve of the corrected brightness of ELISA of HBsAg over a concentration range of  $34 \times 10^1$  to  $34 \times 10^7$  pg/mL ( $n = 8$ ).

the calibration curve of HBsAg on surface-modified PMMA (method #2) was linear over the range of  $34 \times 10^1$  to  $34 \times 10^6$  pg/mL with a regression curve of  $y = 16.46 \log(x) + 74.9$  ( $R^2 = 0.98$ ). The LOD of HBsAg on surface-modified PMMA (method #2) was found to be 160.0 pg/mL (Fig. S3). As observed in both IgG and HBsAg detection, the LOD for both the modification methods were similar, but modification method #1 was more time efficient (1 h) compared to modification method #2 (2 h). Hence, surface modification method #1 was adopted for the subsequent experiments such as HbcAg and multiplexed assays. The LOD of our surface modified device was found to be more sensitive than commercial ELISA kits, HBsAg assay by Yazdani et al. (LOD of 0.7 ng/mL), and our previous hybrid microfluidic device with LOD of 1.3 ng/mL [60,63]. Our LOD was similar to that of the micro-piezoelectric immunoassay by Xu et al. (LOD of 0.1 ng/mL), which however required class-100 clean room and impedance analyzer [64].

For colorimetric ELISA of HbcAg, different concentrations of 10-fold diluted HbcAg ranging from 0.1 ng/mL to 10  $\mu$ g/mL were added to different microwells in the surface-modified PMMA, followed by the addition of anti-HbcAg and ALP-linked IgG. Similar to IgG and HBsAg detection, the intensity of the produced purple color increased from left

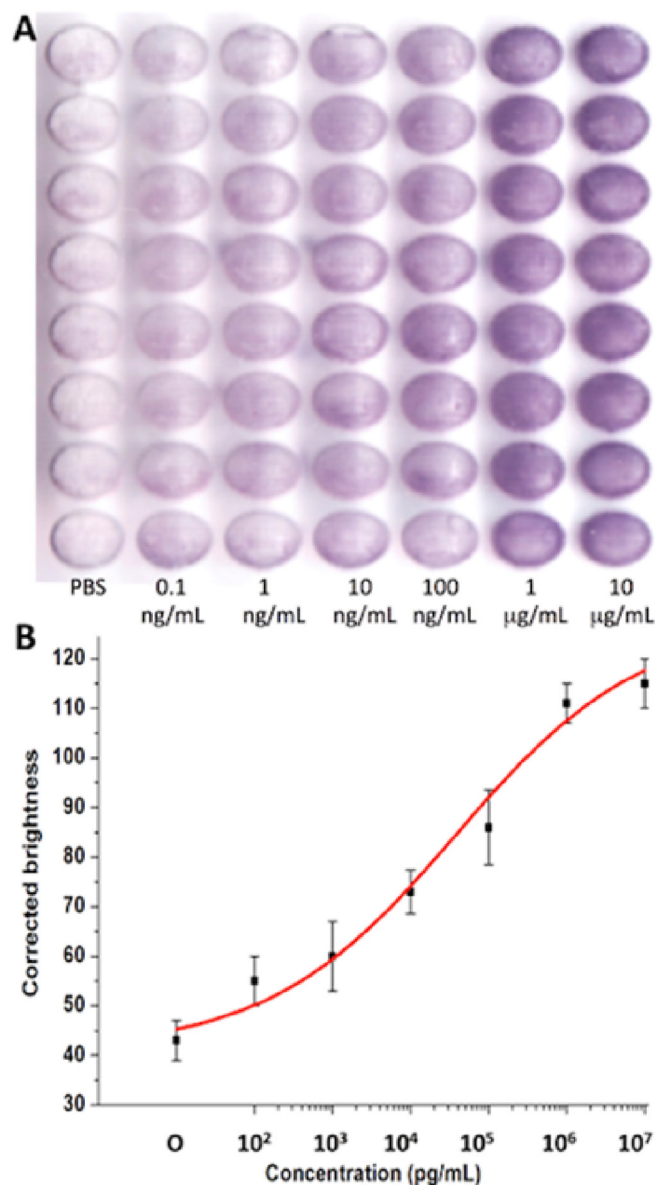


**Fig. 5.** Detection of HBcAg on surface-modified PMMA microplates (Method #1). (A) Scanned image of enzymatic converted substrate in different columns of the microplate with concentrations from left to right: blank (0 pg/mL), 0.1 ng/mL, 1 ng/mL, 10 ng/mL, 100 ng/mL, 1 µg/mL, and 10 µg/mL, respectively. (B) The sigmoidal curve of the corrected brightness of HBcAg over a concentration range of 10<sup>2</sup> to 10<sup>7</sup> pg/mL (n = 8).

to right with corresponding HBcAg concentrations from 0.1 ng/mL to 10 µg/mL (Fig. 5). The calibration curve of HBcAg on surface modified PMMA (method #1) was linear over the range of 10<sup>3</sup> to 10<sup>7</sup> pg/mL with a regression curve of  $y = 14.7 \log(x) + 15.5$  ( $R^2 = 0.98$ ). The LOD of HBcAg on surface-modified PMMA was found to be 300.0 pg/mL.

### 3.4. Multiplexed detection of HBsAg and HBcAg on surface-modified PMMA microdevices

To demonstrate an efficient multiplex biomarker sensing device, the surface-modified PMMA microdevice was used for the simultaneous colorimetric detection of two hepatitis B virus biomarkers- HBsAg and HBcAg. As shown in Fig. 6, the first column was negative control without any antigen, hence no color development. The second and third columns were for the detection of HBsAg while the fourth and fifth columns were for the detection of HBcAg. The third and fourth columns did not develop

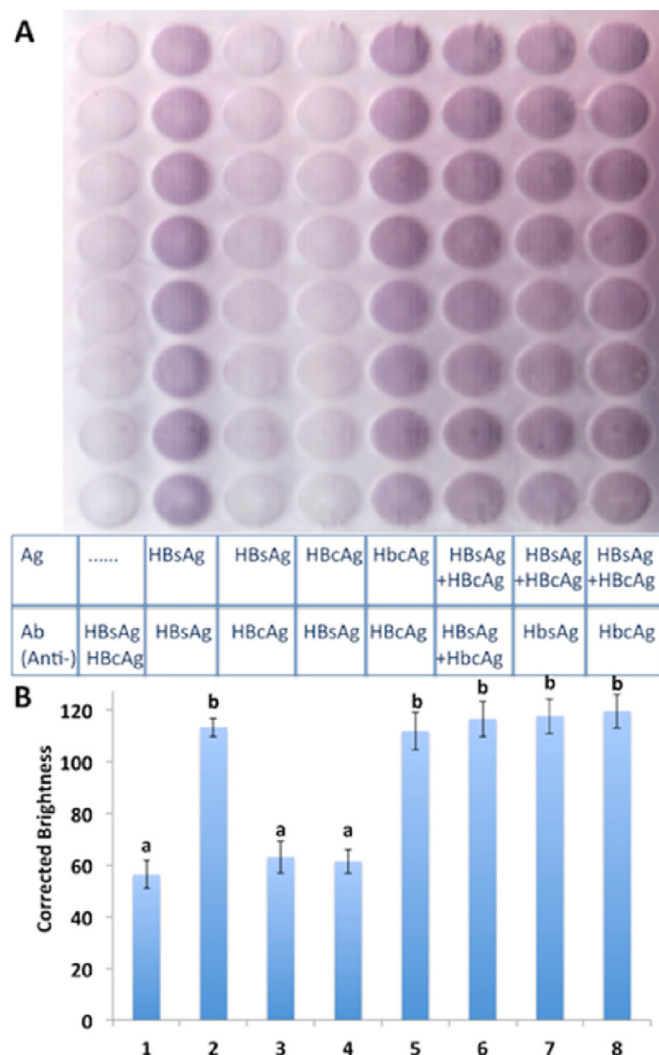


**Fig. 6.** Multiplexed colorimetric ELISA in surface-modified PMMA microdevices. Scanned image of the enzyme-catalyzed substrate (A) and bar plot of the corrected brightness of the scanned image (B) for detection of HBsAg and HBcAg. From left to right: immobilized probe, none (1), HBsAg (2) and (3), HBcAg (4) and (5), and HBsAg + HBcAg (6), (7), and (8), respectively. Test: from left to right, solution containing, anti-HBsAg and anti-HBcAg (1) and (6), HBsAg (2), (4), and (7), and HBcAg (3), (5), and (8). "a" and "b" show that the data are significantly different from each other at  $p \leq 0.05$  (n = 8).

color, as they did not have the respective antibody against the antigen, but the second and fifth columns developed purple as they had their respective antibody. This can also serve as the specificity test, as HBsAg can only bind to anti-HBsAg (2nd column) and not the anti-HBcAg (3rd column). The sixth, seventh, and eighth columns had both the antigen i.e. HBsAg and HBcAg; all of them developed color as they have their respective antibody or the mixture of both antibodies.

### 4. Conclusions

In summary, we have developed a novel polylysine surface modification method to functionalize PMMA surface for enhanced covalent binding of proteins to perform an ultrasensitive immunoassay for multiplexed detection of infectious diseases biomarkers. Specifically, amine-dense polylysine was used to introduce the amine group onto the PMMA surface while the glutaraldehyde acted as a cross-linker ultimately increasing the immobilization efficiency of the protein within a short period of time (20 min compared to overnight incubation in traditional methods). The surface-modified PMMA microfluidic microplate was able

to significantly enhance the sensitivity of the assay without using specialized instruments. LODs of 200.0, 180.0, and 300.0 pg/mL were obtained for IgG, HBsAg, and HbCag, respectively, which were about 10-fold more sensitive than other reported traditional microplate reader-based methods. A wide linear range of detection was also observed in addition to dramatically reduced reagent consumption and a much shorter assay time of 90 min. The basic microplate used here can perform  $8 \times 8$  assays but the design can be simply modified to perform as many experiments and repeats as desired. Additionally, the developed immunoassay meets the ASSURED criteria, which is essential for diagnostics in resource-limited settings. Proof-of-concept testing of the microfluidic microplate was mainly demonstrated using samples prepared in buffer solutions. The microplate's efficacy in real-world clinical settings would need to be further validated using clinical patient samples in order to study large scale cohorts in the future. The study may lead to a simple, rapid, ultrasensitive, and point-of-care device for the simultaneous detection of multiple panels of low-concentration biomarkers in a very low sample volume of different body fluids including saliva, tear, urine or serum. Considering the broad applicability of the microfluidic microplate platform across diverse fields, we envision that the surface-modified PMMA microplate holds tremendous potential as a POC multiplexed testing platform for many applications ranging from clinical diagnosis and biochemical assay to environmental monitoring, particularly in resource-limited settings.

#### CRedit authorship contribution statement

**Sharma T. Sanjay:** Writing – original draft, Validation, Methodology, Investigation, Formal analysis, Data curation. **Sapna Kannan:** Writing – review & editing, Formal analysis. **XiuJun Li:** Writing – review & editing, Visualization, Validation, Supervision, Resources, Project administration, Methodology, Investigation, Funding acquisition, Formal analysis, Conceptualization.

#### Notes

XL and SST have submitted a patent application.

#### Declaration of competing interest

XL and SST have submitted a patent application.

#### Acknowledgements

We would like to acknowledge financial support from NIH/NIAID (R41AI162477), the U.S. NSF (IIP2122712 and CHE2216473), the Cancer Prevention and Research Institute of Texas (CPRI; RP210165), the TTUHSC-UTEP Joint Seed Grant, and the AAFS Foundation Research Lucas grant. We are also grateful for the prior financial support to our research from the NIH/NIAID (R21AI107415), the NIH/NIGMS (SC2GM105584), the NIH/NIMHD RCMI Pilot grant (5G12MD007593-22), the NIH Building Scholar Summer Sabbatical Award, the NSF (IIP1953841, IIP2052347, and DMR1827745), the DOT (CARTEEH), the Philadelphia Foundation, the Medical Center of the Americas Foundation (MCA), the University of Texas (UT) System for the STARS award, and the UTEP for IDR, URI, and MRAP awards.

#### Appendix A. Supplementary data

Supplementary data to this article can be found online at <https://doi.org/10.1016/j.asems.2025.100142>.

#### References

- [1] Y. Lu, Q. Yang, T. Ran, G. Zhang, W. Li, P. Zhou, J. Tang, M. Dai, J. Zhong, H. Chen, P. He, A. Zhou, B. Xue, J. Chen, J. Zhang, S. Yang, K. Wu, X. Wu, M. Tang, W.K. Zhang, D. Guo, X. Chen, H. Chen, J. Shang, Discovery of orally bioavailable SARS-CoV-2 papain-like protease inhibitor as a potential treatment for COVID-19, *Nat. Commun.* 15 (2024) 10169.
- [2] R. Lozano, M. Naghavi, K. Foreman, S. Lim, K. Shibuya, V. Aboyans, J. Abraham, T. Adair, R. Aggarwal, S.Y. Ahn, Global and regional mortality from 235 causes of death for 20 age groups in 1990 and 2010: A systematic analysis for the Global Burden of Disease Study 2010, *The Lancet* 380 (2012) 2095–2128.
- [3] C. Dye, After 2015: Infectious diseases in a new era of health and development, *Phil. Trans. R. Soc. B* 369 (2014) 20130426.
- [4] R.E. Baker, A.S. Mahmud, L.F. Miller, M. Rajeev, F. Rasambainarivo, B.L. Rice, S. Takahashi, A.J. Tatem, C.E. Wagner, L.-F. Wang, Infectious disease in an era of global change, *Nat. Rev. Microbiol.* 20 (2022) 193–205.
- [5] D. Najjar, J. Rainbow, S. Sharma Timilsina, P. Jolly, H. De Puig, M. Yafia, N. Durr, H. Sallum, G. Alter, J.Z. Li, A lab-on-a-chip for the concurrent electrochemical detection of SARS-CoV-2 RNA and anti-SARS-CoV-2 antibodies in saliva and plasma, *Nat. Biomed. Eng.* 6 (2022) 968–978.
- [6] A. Casadevall, Crisis in infectious diseases: 2 decades later, *Clin. Infect. Dis.* 64 (2017) 823–828.
- [7] C. Li, W. Zhou, A.G. Ruiz, Y. Mohammadi, Q. Li, S. Zhang, X. Li, G. Fu, Microfluidic immunoassays for point-of-care testing of SARS-CoV-2 antigens and antibodies, *TrAC, Trends Anal. Chem.* 177 (2024) 117809.
- [8] S.S. Timilsina, N. Durr, P. Jolly, D.E. Ingber, Rapid quantitation of SARS-CoV-2 antibodies in clinical samples with an electrochemical sensor, *Biosens. Bioelectron.* 223 (2023) 115037.
- [9] D. Ganem, A.M. Prince, Hepatitis B virus infection—natural history and clinical consequences, *N. Engl. J. Med.* 350 (2004) 1118–1129.
- [10] C. Trépo, H.L. Chan, A. Lok, Hepatitis B virus infection, *Lancet* 384 (2014) 2053–2063.
- [11] V. Soriano, V. Moreno-Torres, A. Treviño, F. de Jesús, O. Corral, C. de Mendoza, Prospects for controlling hepatitis B globally, *Pathogens* 13 (2024) 291.
- [12] C.L. Lai, V. Ratziu, M.-F. Yuen, T. Poynard, Viral hepatitis B, *Lancet* 362 (2003) 2089–2094.
- [13] X. Li, C. Yang, Analytical chemistry for infectious disease detection and prevention, *Anal. Bioanal. Chem.* 413 (2021) 4561–4562.
- [14] G. Fu, S.T. Sanjay, X. Li, Cost-effective and sensitive colorimetric immunosensing using an iron oxide-to-Prussian blue nanoparticle conversion strategy, *Analyst* 141 (2016) 3883–3889.
- [15] K. Shah, P. Maghsoudlou, Enzyme-linked immunosorbent assay (ELISA): The basics, *Br. J. Hosp. Med.* 77 (2016) C98–C101.
- [16] S.S. Timilsina, X. Li, A paper-in-polymer-pond (PiPP) hybrid microfluidic microplate for multiplexed ultrasensitive detection of cancer biomarkers, *Lab Chip* 24 (2024) 4962–4973.
- [17] S.S. Timilsina, M. Ramasamy, N. Durr, R. Ahmad, P. Jolly, D.E. Ingber, Biofabrication of multiplexed electrochemical immunosensors for simultaneous detection of clinical biomarkers in complex fluids, *Adv. Healthcare Mater.* 11 (2022) 2200589.
- [18] G. Fu, S.T. Sanjay, M. Dou, X. Li, Nanoparticle-mediated photothermal effect enables a new method for quantitative biochemical analysis using a thermometer, *Nanoscale* 8 (2016) 5422–5427.
- [19] J. Kai, A. Puntambekar, N. Santiago, S.H. Lee, D.W. Sehy, V. Moore, J. Han, C.H. Ahn, A novel microfluidic microplate as the next generation assay platform for enzyme linked immunoassays (ELISA), *Lab Chip* 12 (2012) 4257–4262.
- [20] G. Shen, Y. Zhang, Highly sensitive electrochemical stripping detection of hepatitis B surface antigen based on copper-enhanced gold nanoparticle tags and magnetic nanoparticles, *Anal. Chim. Acta* 674 (2010) 27–31.
- [21] S.S. Timilsina, N. Durr, M. Yafia, H. Sallum, P. Jolly, D.E. Ingber, Ultrarapid method for coating electrochemical sensors with antifouling conductive nanomaterials enables highly sensitive multiplexed detection in whole blood, *Adv. Healthcare Mater.* 11 (2022) 2102244.
- [22] S.S. Timilsina, P. Jolly, N. Durr, M. Yafia, D.E. Ingber, Enabling multiplexed electrochemical detection of biomarkers with high sensitivity in complex biological samples, *Accounts Chem. Res.* 54 (2021) 3529–3539.
- [23] S. Shrivastava, T.Q. Trung, N.-E. Lee, Recent progress, challenges, and prospects of fully integrated mobile and wearable point-of-care testing systems for self-testing, *Chem. Soc. Rev.* 49 (2020) 1812–1866.
- [24] W. Zhou, K. Hu, S. Kwee, L. Tang, Z. Wang, J. Xia, X. Li, Gold nanoparticle aggregation-induced quantitative photothermal biosensing using a thermometer: A simple and universal biosensing platform, *Anal. Chem.* 92 (2020) 2739–2747.
- [25] H. Tavakoli, S. Mohammadi, X. Li, G. Fu, X. Li, Microfluidic platforms integrated with nano-sensors for point-of-care bioanalysis, *TrAC, Trends Anal. Chem.* 157 (2022) 116806.
- [26] L. Ma, Y. Abugalyon, X. Li, Multicolorimetric ELISA biosensors on a paper/polymer hybrid analytical device for visual point-of-care detection of infection diseases, *Anal. Bioanal. Chem.* 413 (2021) 4655–4663.
- [27] W. Zhou, G. Fu, X. Li, Detector-free photothermal bar-chart microfluidic chips (PT-Chips) for visual quantitative detection of biomarkers, *Anal. Chem.* 93 (2021) 7754–7762, 7710.1021/acs.analchem.7751c01323.
- [28] M. Dou, N. Macias, F. Shen, J. Dien Bard, D.C. Dominguez, X. Li, Rapid and accurate diagnosis of the respiratory disease pertussis on a point-of-care biochip, *EclinicalMedicine* 8 (2019) 72–77.
- [29] X. Wei, W. Zhou, S.T. Sanjay, J. Zhang, Q. Jin, F. Xu, D.C. Dominguez, X. Li, Multiplexed instrument-free bar-chart SpinChip integrated with nanoparticle-mediated magnetic aptasensors for visual quantitative detection of multiple pathogens, *Anal. Chem.* 90 (2018) 9888–9896.
- [30] H. Tavakoli, E. Hirth, M. Luo, S.S. Timilsina, M. Dou, D.C. Dominguez, X. Li, A microfluidic fully paper-based analytical device integrated with loop-mediated

- isothermal amplification and nano-biosensors for rapid, sensitive, and specific quantitative detection of infectious diseases, *Lab Chip* 22 (2022) 4693–4704.
- [31] J. Zhang, H. Tavakoli, L. Ma, X. Li, L. Han, X. Li, Immunotherapy discovery on tumor organoid-on-a-chip platforms that recapitulate the tumor microenvironment, *Adv. Drug Deliv. Rev.* 187 (2022) 114365.
- [32] S.T. Sanjay, G. Fu, M. Dou, F. Xu, R. Liu, H. Qi, X. Li, Biomarker detection for disease diagnosis using cost-effective microfluidic platforms, *Analyst* 140 (2015) 7062–7081.
- [33] S. T Sanjay, M. Dou, G. Fu, F. Xu, X. Li, Controlled drug delivery using microdevices, *Curr. Pharm. Biotechnol.* 17 (2016) 772–787.
- [34] S.T. Sanjay, W. Zhou, M. Dou, H. Tavakoli, L. Ma, F. Xu, X. Li, Recent advances of controlled drug delivery using microfluidic platforms, *Adv. Drug Deliv. Rev.* 128 (2018) 3–28.
- [35] X.J. Li, Y. Zhou, *Microfluidic devices for biomedical applications*, 1st ed., Elsevier, Oxford, 2013.
- [36] H. Tavakoli, W. Zhou, L. Ma, S. Perez, A. Ibarra, F. Xu, S. Zhan, X. Li, Recent advances in microfluidic platforms for single-cell analysis in cancer biology, diagnosis and therapy, *TrAC, Trends Anal. Chem.* 117 (2019) 13–26.
- [37] A. Bein, C.W. Fadel, B. Swenor, W. Cao, R.K. Powers, D.M. Camacho, A. Naziripour, A. Parsons, N. LoGrande, S. Sharma, Nutritional deficiency in an intestine-on-a-chip recapitulates injury hallmarks associated with environmental enteric dysfunction, *Nat. Biomed. Eng.* 6 (2022) 1236–1247.
- [38] G. Goyal, P. Prabhala, G. Mahajan, B. Bausk, T. Gilboa, L. Xie, Y. Zhai, R. Lazarovits, A. Mansour, M.S. Kim, Ectopic lymphoid follicle formation and human seasonal influenza vaccination responses recapitulated in an organ-on-a-chip, *Adv. Sci.* 9 (2022) 2103241.
- [39] G. Mahajan, E. Doherty, T. To, A. Sutherland, J. Grant, A. Junaid, A. Gulati, N. LoGrande, Z. Izadifar, S.S. Timilsina, Vaginal microbiome-host interactions modeled in a human vagina-on-a-chip, *Microbiome* 10 (2022) 201.
- [40] W. Zhou, M. Dou, S.S. Timilsina, F. Xu, X. Li, Recent innovations in cost-effective polymer and paper hybrid microfluidic devices, *Lab Chip* 21 (2021) 2658–2683.
- [41] M. Dou, S.T. Sanjay, M. Benhabib, F. Xu, X. Li, Low-cost bioanalysis on paper-based and its hybrid microfluidic platforms, *Talanta* 145 (2015) 43–54.
- [42] M. Dou, S.T. Sanjay, D.C. Dominguez, P. Liu, F. Xu, X. Li, Multiplexed instrument-free meningitis diagnosis on a polymer/paper hybrid microfluidic biochip, *Biosens. Bioelectron.* 87 (2017) 865–873.
- [43] A.W. Martinez, S.T. Phillips, G.M. Whitesides, E. Carrilho, *Diagnostics for the Developing World: Microfluidic Paper-Based Analytical Devices*, ACS Publications, 2009.
- [44] W. Zhou, M. Feng, A. Valadez, X. Li, One-step surface modification to graft DNA codes on paper: the method, mechanism, and its application, *Anal. Chem.* 92 (2020) 7045–7053.
- [45] C.M. Cheng, A.W. Martinez, J. Gong, C.R. Mace, S.T. Phillips, E. Carrilho, K.A. Mirica, G.M. Whitesides, paper-based elisa, *Angew. Chem. Int. Ed.* 49 (2010) 4771–4774.
- [46] M. Dou, S.T. Sanjay, D.C. Dominguez, S. Zhan, X. Li, A paper/polymer hybrid CD-like microfluidic SpinChip integrated with DNA-functionalized graphene oxide nanosensors for multiplex qLAMP detection, *Chem. Commun.* 53 (2017) 10886–10889.
- [47] S. Hosseini, F. Ibrahim, I. Djordjevic, L.H. Koole, Recent advances in surface functionalization techniques on polymethacrylate materials for optical biosensor applications, *Analyst* 139 (2014) 2933–2943.
- [48] S.T. Sanjay, M. Li, W. Zhou, X. Li, X. Li, A reusable PMMA/paper hybrid plug-and-play microfluidic device for an ultrasensitive immunoassay with a wide dynamic range, *Microsyst. Nanoeng.* 6 (2020) 28.
- [49] F. Darain, M.A. Wahab, S.C. Tjin, Surface activation of poly (methyl methacrylate) by plasma treatment: Stable antibody immobilization for microfluidic enzyme-linked immunosorbent assay, *Anal. Lett.* 45 (2012) 2569–2579.
- [50] Y. Bai, C.G. Koh, M. Boreman, Y.-J. Juang, I.-C. Tang, L.J. Lee, S.-T. Yang, Surface modification for enhancing antibody binding on polymer-based microfluidic device for enzyme-linked immunosorbent assay, *Langmuir* 22 (2006) 9458–9467.
- [51] W. Zhou, J. Sun, X. Li, Low-cost quantitative photothermal genetic detection of pathogens on a paper hybrid device using a thermometer, *Anal. Chem.* 92 (2020) 14830–14837.
- [52] L. Brown, T. Koerner, J.H. Horton, R.D. Oleschuk, Fabrication and characterization of poly (methylmethacrylate) microfluidic devices bonded using surface modifications and solvents, *Lab Chip* 6 (2006) 66–73.
- [53] S.L. Llopis, J. Osiri, S.A. Soper, Surface modification of poly (methyl methacrylate) microfluidic devices for high-resolution separations of single-stranded DNA, *Electrophoresis* 28 (2007) 984–993.
- [54] Y. Liu, H. Wang, J. Huang, J. Yang, B. Liu, P. Yang, Microchip-based ELISA strategy for the detection of low-level disease biomarker in serum, *Anal. Chim. Acta* 650 (2009) 77–82.
- [55] S. Sui, L. Li, J. Shen, G. Ni, H. Xie, Q. Lin, Y. Zhao, J. Guo, W. Duan, Plasma treatment of polymethyl methacrylate to improve surface hydrophilicity and antifouling performance, *Polym. Eng. Sci.* 61 (2021) 506–513.
- [56] G. Duan, C. Zhang, A. Li, X. Yang, L. Lu, X. Wang, Preparation and characterization of mesoporous zirconia made by using a poly (methyl methacrylate) template, *Nanoscale Res. Lett.* 3 (2008) 118.
- [57] D.M. Wingerchuk, B. Banwell, J.L. Bennett, P. Cabre, W. Carroll, T. Chitnis, J. De Seze, K. Fujihara, B. Greenberg, A. Jacob, International consensus diagnostic criteria for neuromyelitis optica spectrum disorders, *Neurology* 85 (2015) 177–189.
- [58] N.M. van Gerven, Y.S. de Boer, C.J. Mulder, C.M. van Nieuwkerk, G. Bouma, Auto immune hepatitis, *World J. Gastroenterol.* 22 (2016) 4651.
- [59] S. Zhang, A. Garcia-D'Angeli, J.P. Brennan, Q. Huo, Predicting detection limits of enzyme-linked immunosorbent assay (ELISA) and bioanalytical techniques in general, *Analyst* 139 (2014) 439–445.
- [60] S.T. Sanjay, M. Dou, J. Sun, X. Li, A paper/polymer hybrid microfluidic microplate for rapid quantitative detection of multiple disease biomarkers, *Sci. Rep.* 6 (2016) 30474.
- [61] N.B. Slama, S.S. Ahmed, F. Zoulim, Quantification de l'antigène HBs: Signification virologique, *Gastroentérol. Clin. Biol.* 34 (2010) S112–S118.
- [62] J. Jaroszewicz, B.C. Serrano, K. Wursthorn, K. Deterding, J. Schlue, R. Raupach, R. Flisiak, C.-T. Bock, M.P. Manns, H. Wedemeyer, Hepatitis B surface antigen (HBsAg) levels in the natural history of hepatitis B virus (HBV)-infection: A European perspective, *J. Hepatol.* 52 (2010) 514–522.
- [63] Y. Yazdani, A. Roohi, J. Khoshnoodi, F. Shokri, Development of a sensitive enzyme-linked immunosorbent assay for detection of hepatitis B surface antigen using novel monoclonal antibodies, *Avicenna J. Med. Biotechnol. (AJMB)* 2 (2010) 207.
- [64] T. Xu, J. Miao, Z. Wang, L. Yu, C.M. Li, Micro-piezoelectric immunoassay chip for simultaneous detection of Hepatitis B virus and  $\alpha$ -fetoprotein, *Sensor. Actuator. B Chem.* 151 (2011) 370–376.